26th INTERNATIONAL CONGRESS ON SOUND AND VIBRATION
7-11 July 2019, Montreal

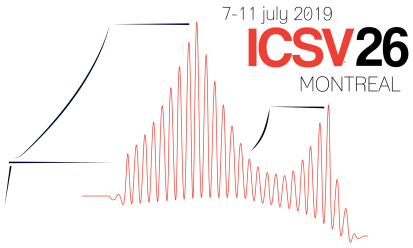

OPTIMIZATION OF METASURFACES FOR THE DESIGN OF NOISE TRAPPING METADEVICES

Umberto Iemma
Università degli Studi Roma Tre, Roma, Italia
email: umberto.iemma@uniroma3.it

Giorgio Palma
Università degli Studi Roma Tre, Roma, Italia
email: giorgio.palma@uniroma3.it

The article deals with the design of a metadevice able to trap acoustic waves in a duct. The acoustic perturbation is produced by a source placed inside the duct. The aim is to limit the outgoing acoustic power and confine the perturbation inside the duct exploiting the unconventional reflection of the optimized metasurface. The metabehaviour is modeled by means of the generalized Snell's law for reflection from acoustically rigid surfaces. The realization of the device relies on a modular concept, which building set is made of eight elementary cells, able to induce a reflected field suitably phase-delayed with respect to the incident wave. The set spans the whole 0-2π phase delay range, and the anomalous reflection is obtained by the tailored design of the phase delay gradient profile on the metasurface. The cells are designed in order to extend the effective frequency range of the device, keeping the overall thickness of the metadevice smaller than a quarter of the design wavelength. The duct and the source are considered co–moving within the fluid at rest. The numerical analysis is performed in the frequency domain in a frame of reference rigidly connected to the duct, and considering several values for the Mach number.
Keywords: metamaterials, aeroacoustics, optimization, spacecoiling

1. Introduction

During the last fifteen years, metamaterials have been object of great interest by the research community in several fields. Scientific contributions regarding acoustic metamaterials have grown in number almost exponentially just considering the last three years. A possible interpretation of the word metamaterial can be extrapolated merging various definitions that have been formulated since 1999 [1], stating that a metamaterial is a macroscopic composite of periodic or non–periodic cellular architecture designed to produce an optimized response, not available in nature or difficult to obtain otherwise, to a specific excitation. Its functionality is due more to its particularly engineered architecture and microstructure than to its chemical composition, and the response of properly defined unit cells can be translated into averaged effective parameters defining a metacontinuum. This definition, and so the similar others that can be found in literature, have wide boundaries, allowing for very different approaches to the design of metamaterials. Among the others, famous are the coordinate transformation approach borrowed from early

studies of metamaterials in electromagnetism by Pendry [2] and Leonhardt [3], that led to the formalization of the so–called acoustic cloaking [4, 5, 6], and its variant called carpet cloaking firstly proposed by Cummer and Shurig [7], *i.e.* the definition of a metafluid that, when placed around an object, is capable to bend the incoming acoustic perturbation around the obstacle, preventing its scattering and hence making it acoustically "invisible". Recently, research is aiming at the extension of the theory of cloaking [8, 9, 10], and in general of coordinate transformation [11, 12, 13] to the aeroacoustic domain, at least for subsonic potential flows, overcoming the previous limitations of applicability to quiescent fluids; however, literature on the subject is still really small compared to huge amount of works on quiescent fluids. The exploitation of resonance and antiresonance effects is another extensively adopted method to induce metabehaviours, leading to materials exposing effective negativity in density and/or bulk modulus, potentially preventing transmission (single negativity) [14] of the acoustic waves or enabling an inverse energy flow (double negativity) [15]. This so induced metabehaviours are tipically narrow band, due to the nature of the underlying resonant phenomenon, and a lot of effort has been put aiming at the extension of the bandwidth of such devices [16, 17]. A complete bibliographic survey is difficult due to the rapidly expanding literature, and anyhow beyond the scope of this article. Interesting review contributions can be found in literature, such as [18]. It's still of interest to mention the remarkable work by [19] in which a way to modify the reflection angle from surfaces impinged by an acoustical perturbation is achieved with a metasurface, *i.e.* a device which overall thickness is subwavelength at the design frequency. The metabehaviour is modeled by means of what goes under the name of "generalized Snell's Law for reflection", that defines an extra contribution to the reflection angle from a metasurface linked to the ability of the latter to induce a phase delay in the propagation of the reflected wave. Designing a suitable phase delay gradient by the metasurface, its reflection angle can be modified at will.
The present work will share the same principle adopted in the mentioned work in order to achieve back reflection within a duct, limiting the outgoing radiation, *i.e.* partially *trapping* the sound. This design is intended to be a first step towards the integration of metamaterial devices in structures of aeronautical interests for community noise mitigation that, in the authors' opinion, will lead to the realization of devices such as virtually scarfed nacelles and/or efficiency improvements of existing acoustic liners, taking advantage of back reflection and sound trapping from the metasurfaces.

Throughout the work a two–dimensional assumption is used. In Sec. 2, after a brief definition of metasurface, the Generalized Snell's Law theory for unconventional reflection is recalled and the metasurface design principles are presented. Section 3 illustrates the numerical setup while details on numerical simulations and their results are shown in Sec.4. Brief concluding considerations can be found in Sec.5.

2. Metasurface design

A metasurface can be defined as a metamaterial device built with an overall thickness (deeply) below the working wavelength. A thin design is often desirable for a metamaterial as this allows its applicability in a broader range of real applications, hence explaining the great interest in the development of metasurfaces. A considerable part of literature is focused on the so called *space–coiling* design, in which acoustic wave guides, bent to coil up their extension, are exploited to induce a metabehaviour. The majority of applications that aim at obtaining anomalous reflection or refraction properties are based on that concept, *e.g.*, lens–behaving [20] or arbitrarily-shaped virtual surfaces [21] The underlying theory is based on the generalized Snell's law for acoustic reflection and refraction, that stems out from its analogous in optics [22]:

$$\sin\theta_r(x,\omega) = \frac{\lambda}{2\pi}\frac{\partial\phi(x,\omega)}{\partial x} + \sin\theta_i(x,\omega), \qquad \sin\theta_t(x,\omega) = \frac{\lambda}{2\pi}\frac{\partial\phi(x,\omega}{\partial x}) + \sin\theta_i(x,\omega) \tag{1}$$

where λ is the wavelength of the incident wave, θ_i is the angle between the direction of propagation and the metasurface, θ_r is the reflection angle, and θ_t is the refraction angle, while ϕ is the phase delay between the reflected/refracted and the impinging wave. This equations link the extraordinary reflection/refraction behaviour with the presence of a gradient of induced phase delay in the reflected/refracted wave on the metasurface; when there is no induced phase gradient on the surface the relation between incident and reflected wave is, as expected, described by the traditional Snell's law. All the cited works share a common approach: the 0-2π phase delay range is quantized and approximated by a piecewise function with an arbitrary number of steps, hence elementary cells in the same number are designed, each one inducing a suitable different phase shift in the acoustic reflected or transmitted field. Those are then combined as *bricks* of the metasurface to reproduce (approximately) the needed phase delay gradient profile which has been analytically derived from a desired spacial distribution of the reflected/refracted angle over the metasurface.
In this paper we follow the same path to develop a generalized Snell's law metasurface for extraordinary reflection. This will be placed on the walls of a duct to limit the outgoing radiation, partially trapping inside the duct the acoustic waves incoming from the inside by means of back reflection from the metasurface. In particular, the metasurface would change the radiation pattern of the duct, and it is intended to limit the emission towards areas above and below the duct itself.

To analytically evaluate a optimum target profile of phase shift gradient over the metasurface, the incident acoustic field must be known *a–priori* in terms of incident angle, tailoring in this way the metasurface to the specific application. Here, we renounce to the exact calculation of the actual reflected angle from the metasurface; in fact, the resulting device is intended to be effective in a wide range of operational situations, *e.g.* with different incident acoustic fields and convective speeds, at the price that the final performances of the device will not be the best theoretically achievable. For this reason the metasurface is designed to give a constant spatial distribution of extra reflection angle to the acoustic incident perturbation of 90^o.

The building set for the metasurface is composed by eight unit cells, able to cover the whole 0-2π range with equally spaced phase delays, evaluated as the phase of the reflection coefficient R of the cell $\phi = \arg(R) = \tan^{-1}(\frac{\mathcal{I}(R)}{\mathcal{R}(R)})$. Four parameters, together with the choice of the design operating frequency (f^*), completely define the elementary cell, depicted in Fig. 1:

- a_x - maximum cell depth = $\lambda^*/8$;
- a_y - cell width = $\lambda^*/8$;
- d - neck width;
- l_n - neck length;
- h_c - cavity width;
- h_l - cavity depth;

Following [17], the constructive parameters of each cell have been optimized: the effective bandwidth of a metasurface built with those cells is extended minimizing the variability of the metasurface $\nabla(\phi)$ with respect to the working frequency: in the cited work it is shown how the resulting device is able to steer the reflected field effectively up to $f_{max} \sim 1.4f^*$. As can be seen in Fig.1, cells have the typical shape of Helmholtz resonators, however an eigenfrequency analysis of the optimized cells shows clearly that the metasurface is not exploiting resonance, as the frequency range under consideration is far away from the resonance of the cells, see Table 1. Equation (1) is used to define the analytic phase delay profile, shown in Fig. 2b along with its approximation achieved by the so–defined cells for the design frequency. The obtained metasurface is modular, *i.e.* a surface of arbitrary extension can be designed simply repeating the metasurface unit of Fig. 2a composed by eight cells, as the phase delay gradient

profile would be continuous.

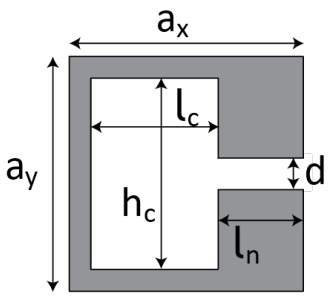

Figure 1: Unit cell parametrization.

Cell #	1^{st} resonance frequency
1	8.45 f^*
2	4.38 f^*
3	4.36 f^*
4	4.37 f^*
5	4.39 f^*
6	4.4 f^*
7	4.4 f^*
8	3.82 f^*

Table 1: 1^{st} resonance frequencies of optimized cells.

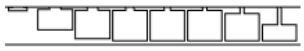

(a)

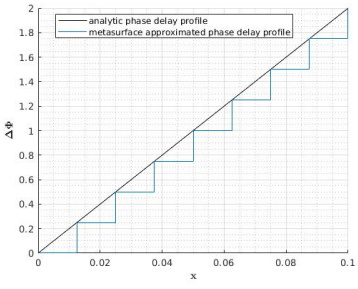

(b)

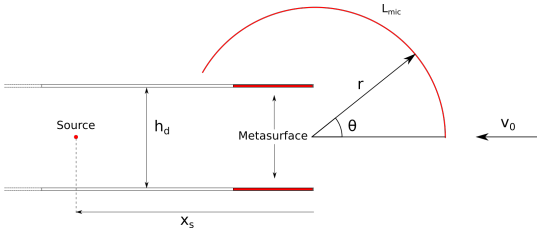

(c)

Figure 2: (a) The optimized metasurface unit, composed by eight elementary cells giving extra 90^o reflection angle by means of phase delay gradient. (b) Analytic target phase delay profile along one unit of metasurface and the approximation reached by the metasurface. (c) Sound trapping setup: two metamaterial tiles are placed symmetrically at the inlet of a duct. The hosting fluid is moving with uniform velocity $\mathbf{v}_0$.

3. Sound trapping setup

The setup is sketched in Fig. (2c): an elementary acoustic point source is placed inside a duct which is in turn in a unbounded domain. The metasurface device depicted in Sec.2 is designed for a nominal operating frequency $f^* = 3430$ Hz and it is arranged symmetrically on a subsection of the upper and lower duct walls, using six metasurface units (of eight suitably arranged cells each) per side up to (near to) the inlet section. The effect of the metasurface is investigated using a two–dimension approximation, so that the duct dimensions are defined by its height $h_d = 0.775$ m as it is considered infinitely long, and the source is placed on the duct symmetry line at $x_s = 1.8$ m from the inlet section.
The source and the duct, with the metasurface, are immersed in a moving hosting fluid, with a uniform velocity $\mathrm{v}_0 = Mc_0$ directed inside the duct. As a simplifying assumption, the hosting fluid is considered quiescent inside the cells of the metasurface, *i.e.* the metasurface is considered to be aerodynamically impermeable. Some considerations about this can be found in Sec. (5). The acoustic propagation in presence of the vorticity–free flow of a barotropic, inviscid fluid is governed by

$$-\frac{\partial}{\partial t}\left[\frac{\rho_0}{c_0^2}\left(\frac{\partial \varphi}{\partial t}+\mathbf{v}_0\cdot\nabla\varphi\right)\right]+\nabla\cdot\left[\rho_0\nabla\varphi-\frac{\rho_0}{c_0^2}\left(\frac{\partial \varphi}{\partial t}+\mathbf{v}_0\cdot\nabla\varphi\right)\mathbf{v}_0\right]=0 \tag{2}$$

where φ is the acoustic potential, $\mathbf{v}_0$, ρ_0 and c_0 are the mean–flow velocity, local density and speed of sound, respectively. A monochromatic acoustic perturbation is considered to be emitted from the point source and simulations are carried out in frequency domain. The corresponding governing equation can be obtained Fourier transforming Eq.(2). Duct and cells walls are considered to be perfectly hard for the acoustic perturbations.

4. Numerical results

Numerical analyses of the setup described in previous sections are performed using Finite Element Method, the computational domain is hence truncated by means of a radiation condition at the outer boundaries. In addition to the setup described in the previous section, a plain duct with no metasurfaces installed, *i.e.* with all sound–hard flat walls, is taken as reference geometry. A octave band of interest is defined, centered on the design frequency of the metasurface f^* ($f_{min} = f^*/\sqrt{2} = 2425$ Hz, $f_{max} = f^*\sqrt{2} = 4850$ Hz), defining a range in which simulations are performed. To investigate the effects of convection on the efficacy of the metasurface, simulations are carried out for three values of $\mathbf{v}_0$, corresponding to Mach 0.1, 0.2 and 0.3. Defining a polar coordinate system (r, θ) centered at the inlet section on the duct symmetry line (see Fig. 2c), an arc of virtual microphones ($\mathcal{L}_{mic}$) is defined with $r = 1$ m that extends from $0 < \alpha < 150^o$.
The Insertion Loss, defined as

$$\mathrm{IL}(\theta) = 10 \log_{10} \left(\frac{p_{fw}^2}{p_{mm}^2} \right), \tag{3}$$

where p_{fw} and p_{mm} are respectively the pressure field related to the duct with flat hard walls and in presence of the metasurfaces, is identified as a local merit factor of the effect of the metasurface on the pressure field, that related to the modified directivity of the duct.

Polar plot in Fig. 3c shows a neat emission reduction for $\alpha \geq 90^o$. Comparing the pressure field visualization in Fig. 3b with the reference solution in Fig. 3a, it is evident how the metasurface is reflecting back the acoustic perturbation and reducing the diffraction from the duct edge. For some frequencies the IL seems not to confirm this result, like in Fig.3f; analyzing the pressure fields related to this cases (Figs. 3e and 3d), however, it appears that the back reflection from the metasurface is still happening, but the diffraction from the duct edges is very limited also for the flat wall reference case, and using the IL alone as estimator is misleading. The metamaterial device is clearly acting on the field redistributing the acoustic energy, drastically changing the directivity pattern of acoustic emissions of the duct at all the three Mach numbers tested as can be seen in Fig. 4: the homogeneous flow seems to affect marginally the metabehaviour induced.

5. Conclusions

A subwavelenght metamaterial device has been designed starting from its elementary unit cells. Those have been optimized in a robust sense, widening the frequency range of efficacy. Installing this metasurface near the outlet section of a duct, partial sound trapping of the acoustic perturbation from a monopolar point source placed inside the duct is achieved and the acoustic directivity of the duct is changed. Numerical simulations shown the efficacy of the device in a octave band centered in the design frequency of the metasurface, at different Mach numbers of the hosting fluid. Fluid velocity, at least for a homogeneous flow, seems not to affect dramatically the functioning of the spacecoiling–based metadevice in the tested range. In this work the phase delay profile provided by the metasurface was chosen to produce an extra reflection angle of 90^o; also the position and the extension of the metasurface were fixed.

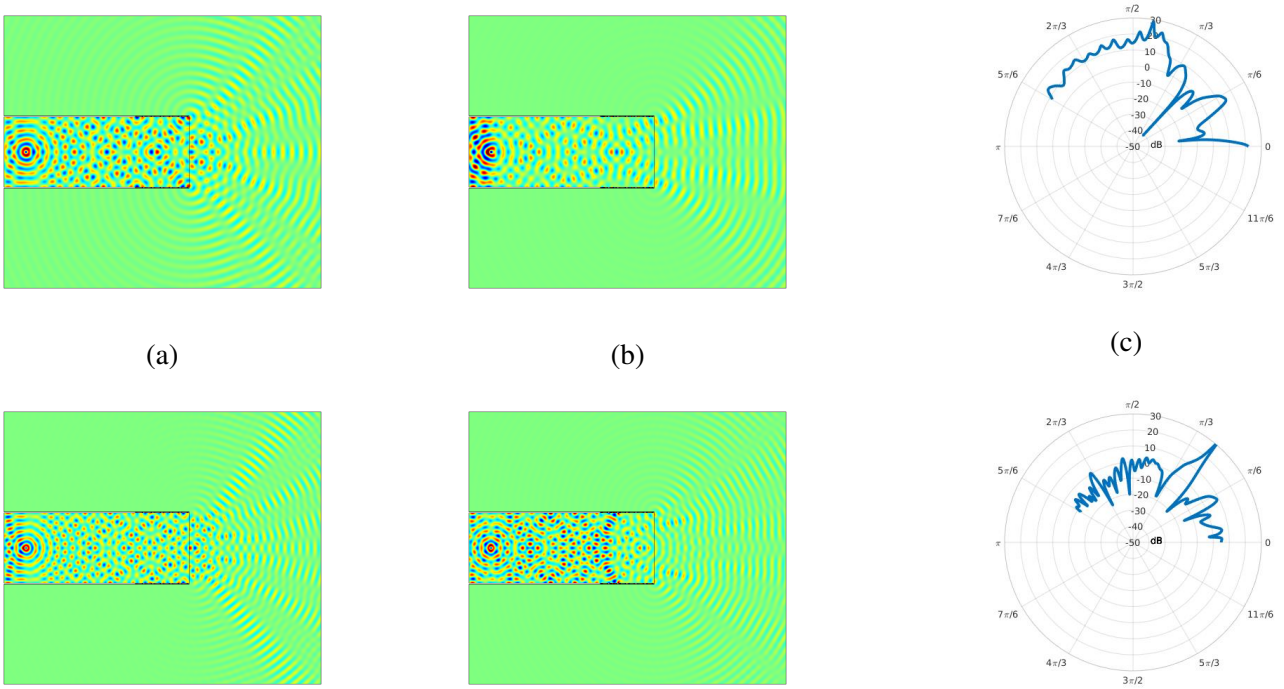

Figure 3: Sound trapping by metasurface, (a,d) pressure field with flat walls, (b,e) pressure field with metasurfaces, (c,f) polar insertion loss at $\mathcal{L}_{mic}$. M = 0.0, f = 3430 and 4230 Hz.

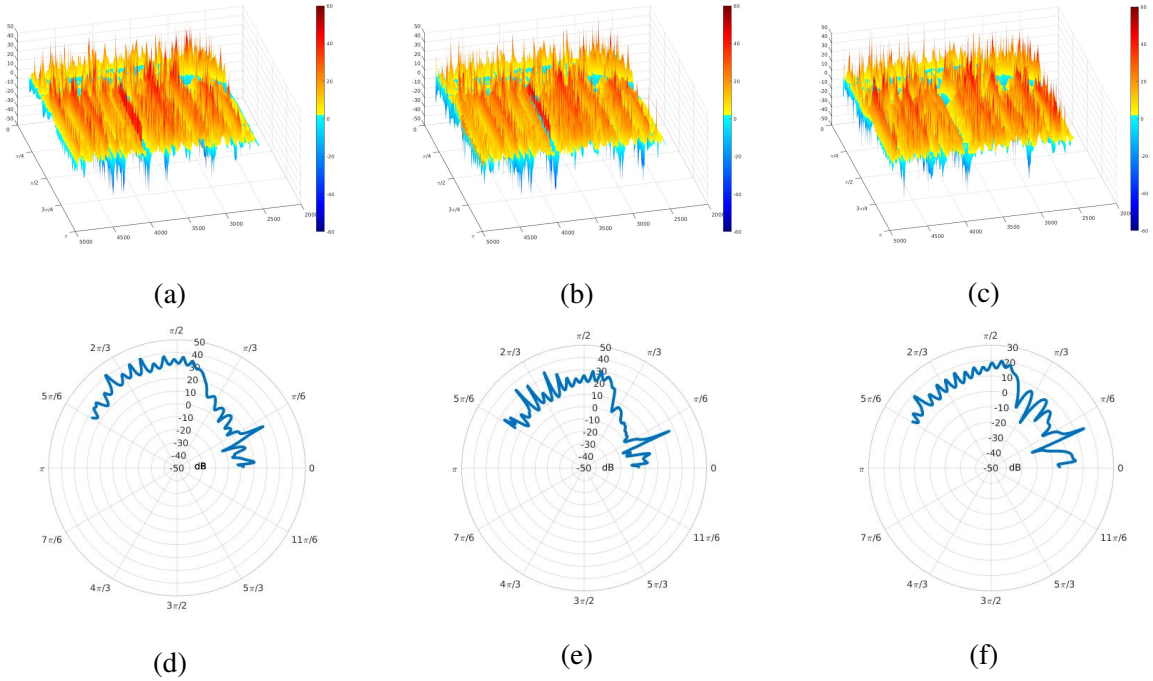

Figure 4: IL maps (a, b, c) in the considered octave band and polar details at 4430 Hz (d, e, f) for M=0.0, M=0.1 and M=0.2

This decision was taken to design a device able to work in as general as possible conditions. However, the above mentioned parameters are degree of freedom for the designer and could be tuned in order to maximize a desired target behaviour given a particular incident acoustic field, for example via numerical optimization.

In Sec. 3 it is stated that in numerical simulations the metasurface has been considered aerodynamically impermeable. This simplifying assumption is clearly not realistic looking at the effective geometry of the device, which presents slits of non negligible size directly exposed to the flow. This would lead to an increase of the drag induced and, even more important, to self noise produced by the metasurface, probably nullifying its noise reduction effect. However, the interaction between the metasurface and the aerodynamic field can be drastically reduced covering the metasurfaces with a thin layer of Kevlar. This solution has been studied in [23] to minimize the effect of the acoustic treatments and section discontinuities on aerodynamic and acoustic measurements in wind tunnels within an anechoic test section. Kevlar layers demonstrated to be almost acoustically transparent (IL due to the Kevlar is always less than 3.5dB) in a wide range of frequencies and were also effective to drastically limit the flow induced background noise due to the interactions between the flow and anechoic treatments and microphone arrays [24]. The assumption in Sec. 3 was made having in mind that, in real applications, the metasurfaces would be covered by a layer of an acoustically transparent material with low porosity, like Kevlar or equivalents.

Acknowledgements

This work has been supported by the European Commission through the Project AERIALIST (AdvancEd aicRaft-noIse-AlLeviation devIceS using meTamaterials), Grant Agreement no. 723367.

REFERENCES

1. Weiglhofer, W. S. and Lakhtakia, A., *Introduction to Complex Mediums for Optics and Electromagnetics*, SPIE Publications (1999).

2. Pendry, J. B., Schurig, D. and Smith, D. Controlling electromagnetic fields., *Science*, **312**, 1780–1782, (2006).

3. Leonhardt, U. Optical conformal mapping., *Science*, **312**, 1777–1780, (2006).

4. Norris, A. Acoustic cloaking theory., *Proceedings of the Royal Society A: Mathematical, Physical and Engineering Sciences*, **464**, 2411–2434, (2008).

5. Norris, A. Acoustic metafluids., *The Journal of the Acoustical Society of America*, **125**, 839–849, (2009).

6. Iemma, U. and Burghignoli, L. An integral equation approach to acoustic cloaking, *Journal of Sound and Vibration*, **331** (21), 4629 – 4643, (2012).

7. Cummer, S. A. and Schurig, D. One path to acoustic cloaking., *New Journal of Physics*, **9**, 45, (2007).

8. Iemma, U., Carley, M. and Pellegrini, R. Tailoring acoustic metamaterials to aeroacoustic applications, *43th International Congress and Exposition on Noise Control Engineering, Inter-noise 2014*, (2014).

9. Iemma, U. Theoretical and numerical modeling of acoustic metamaterials for aeroacoustic applications., *Aerospace*, **3** (2), (2016).

10. Iemma, U. and Palma, G. Aeroacoustic design of metafluid devices, *24th International Congress on Sound and Vibration, ICSV 2017*, (2017).

11. García-Meca, C., Carloni, S., Barceló, C., Jannes, G., Sánchez-Dehesa, J. and Martínez, A. Analogue transformations in physics and their application to acoustics., *Scientific reports*, **3**, 2009, (2013).

12. Iemma, U. and Palma, G. Analogue transformation acoustics in aeronautics, *46th International Congress and Exposition on Noise Control Engineering, Inter-noise 2017*, (2017).

13. Iemma, U. and Palma, G. On the use of the analogue transformation acoustics in aeroacoustics, *Mathematical Problems in Engineering*, **vol. 2017**, 16 pages, article ID 8981731, doi:10.1155/2017/8981731, (2017).

14. Liu, Z., Zhang, X., Mao, Y., Zhu, Y. Y., Yang, Z., Chan, C. T. and Sheng, P. Locally resonant sonic materials, *Science*, **289** (5485), 1734–1736, (2000).

15. Pendry, J. B. Negative refraction makes a perfect lens, *Physical review letters*, **85** (18), 3966, (2000).

16. Zhu, Y.-F., Zou, X.-Y., Li, R.-Q., Jiang, X., Tu, J., Liang, B. and Cheng, J.-C. Dispersionless manipulation of reflected acoustic wavefront by subwavelength corrugated surface, *Scientific Reports*, **5**, 10966, (2015).

17. Palma, G., Cioffi, I., Centracchio, F., Burghignoli, L. and Iemma, U. Steering of acoustic reflection from metasurfaces through numerical optimization, *25th AIAA/CEAS Aeroacoustics Conference (Aeroacoustics 2019)*, American Institute of Aeronautics and Astronautics, (2019).

18. Palma, G., Mao, H., Burghignoli, L., GÃ¶ransson, P. and Iemma, U. Acoustic metamaterials in aeronautics, *Applied Sciences*, **8** (6), (2018).

19. Li, Y., Liang, B., Gu, Z.-m., Zou, X.-y. and Cheng, J.-c. Reflected wavefront manipulation based on ultrathin planar acoustic metasurfaces, *Scientific Reports*, **3**, 2546, (2013).

20. Wang, W., Xie, Y., Konneker, A., Popa, B.-I. and Cummer, S. A. Design and demonstration of broadband thin planar diffractive acoustic lenses, *Applied Physics Letters*, **105** (10), 101904, (2014).

21. Li, Y., Jiang, X., Li, R.-q., Liang, B., Zou, X.-y., Yin, L.-l. and Cheng, J.-c. Experimental realization of full control of reflected waves with subwavelength acoustic metasurfaces, *Phys. Rev. Applied*, **2**, 064002, (2014).

22. Esfahlani, H., Karkar, S., Lissek, H. and Mosig, J. R. Acoustic carpet cloak based on an ultrathin metasurface, *Phys. Rev. B*, **94**, 014302, (2016).

23. Devenport, W., Burdisso, R., Borgoltz, A., Ravetta, P. and Barone, M. Aerodynamic and acoustic corrections for a kevlar-walled anechoic wind tunnel, *16th AIAA/CEAS Aeroacoustics Conference*, American Institute of Aeronautics and Astronautics, (2010).

24. Jaeger, S., Horne, W. and Allen, C. Effect of surface treatment on array microphone self-noise, *6th Aeroacoustics Conference and Exhibit*, American Institute of Aeronautics and Astronautics, (2000).